RESEARCH AND APPLICATIONS IN AEROSERVOELASTICITY AT THE NASA LANGLEY RESEARCH CENTER

Irving Abel and Thomas E. Noll
NASA Langley Research Center
Hampton, Virginia

Abstract

A review of analytical methods used to analyze flexible vehicles with active controls is presented. Methods used to approximate and correct unsteady aerodynamic forces used in the analysis are discussed. Recent advances in the application of optimal methods to digital control law synthesis are presented. The use of active controls in an integrated design process is also discussed. Finally, the results of recent wind-tunnel studies aimed at demonstrating active control concepts and validating the analytical methods are presented.

Introduction

The application of active controls technology to reduce aeroelastic response of aircraft structures offers a potential for significant payoff in terms of aerodynamic efficiency and structural weight savings. In the past, conventional aircraft designs were relatively rigid, had stable flying qualities, exhibited conventional flight dynamics, and had weak couplings between the structure, the rigid body degrees of freedom and the control functions. As new innovative configurations appear, they are tending to be very flexible, have unstable flight modes, and require active controls which can exhibit a strong coupling between the structure and the control functions. New aircraft configurations are now being considered with active controls that would be unacceptable by traditional design standards. To reduce the technical risk associated with active controls technology, research was begun at the NASA Langley Research Center in the late 1960's to advance this concept through a broad-based research program. Included was research in the areas of analysis, synthesis, design, and experimental validation of the methods.

In the broadest sense, "active controls" refers to any control system that senses a deviation from a desired condition and through a feedback action brings the condition back to that desired. In this sense, active controls have been in use on aircraft for over 60 years, starting with the simplest forms of auto pilots that maintained a desired heading and altitude and progressing to systems that control rigid-body aircraft dynamics. A number of tests were performed in England and the United States in the 1950's to investigate gust-alleviation systems that used automated control surfaces to reduce aircraft motions[1,2]. A 33-year old textbook on aeroelasticity[3] speaks of the possibility of flutter suppression by means of a closed-loop automatic control system. With a few exceptions, it was not until the late sixties and early seventies that systems for controlling aircraft structural response were seriously considered.

I. E. Garrick pointed out in his 1976 Von Karman lecture, "a major trend which will play a dominant role in research, development, and practice in the years ahead is the union of modern control technology and aeroelasticity". Although aeroelasticians and control specialists have usually gone their separate ways, and both fields have become quite sophisticated, in the last half dozen years there have been real attempts at cooperation and the adapting to each other's methods. An indication of the growing realization of the importance of active control of aeroelastic response is the coining of the term "aeroservoelasticity" to describe this technology area.

The emergence of active control systems to control aeroelastic response rests partly in design trends which emphasize higher performance and wider mission requirements, and therefore, the need to avoid compromise; partly in improved hardware and computer capability; partly in the growth of confidence by their general use in the space program; and partly due to the research activities and experience gained as part of this NASA research program. Two major drivers related to the emergence of active control technology were the successes that had been achieved in reducing fatigue damage on the B-52 through the limited use of active controls[4] and a significant flutter problem that was encountered during the design phase of the national SST that would have required active controls in lieu of large structural weight increases.

The purpose of this paper is to report on the progress that has been made in aeroservoelasticity at NASA Langley in the last three years. Topics to be covered will include: the development and refinement of analytical tools to synthesize control laws and to analyze flexible vehicles; the results of wind-tunnel studies aimed at demonstrating the concepts and validating the analytical methods; and the application of aeroservoelastic analysis to future flight vehicles. Figure 1 indicates the breadth of the program to be covered in this paper.

Analysis

To take full advantage of active control technology, control law synthesis must be an integral part of the overall aircraft design process. This requires efficient computational methods to enable the designer to routinely analyze complex, controlled aircraft systems. A significant amount of work has been done at NASA Langley to develop analytical tools for this task.

The analysis of an actively controlled flexible aircraft requires that the interfaces among unsteady aerodynamics, structures, and control theory be properly considered. Because of the multidisciplinary nature of the problem, the format of the equations of motion and the analytical methods used to solve them are in many cases inconsistent. For example, the equations of motion for a flexible vehicle in terms of its vibration modes may be expressed in matrix form as

$$\left([M]s^2 + [2\zeta M\Omega]s + [M\Omega^2] + \frac{1}{2}\rho V^2\left[\hat{Q}\right]\right)\{q\} = -\frac{1}{2}\rho V\left\{\hat{Q}_g\right\}w_g \qquad (1)$$

where $\Omega = \begin{bmatrix}\omega_1 & & \\ & \ldots & \\ & & \omega_n\end{bmatrix}$ and ω_i is the i^{th} natural vibration mode frequency; [M], represents the generalized mass matrix;

$[2\zeta M\Omega]$, the structural damping matrix; $[M\Omega^2]$, the generalized stiffness matrix; $[\hat{Q}]$, the complex generalized aerodynamic force matrix (GAF) due to motion; $\{\hat{Q}_g\}$, the complex GAF vector due to vertical gust disturbance; $\{q\}$, the generalized coordinate vector; s, the Laplace transform variable; and ρ, V, and w_g the free stream density, free stream velocity, and the gust velocity, respectively. All matrices are of the size n x (n + r), where n is the number of structural modes and r is the number of active control surfaces (hinge moments equations are neglected). By partitioning the generalized coordinate vector as

$$\{q\} = \begin{Bmatrix} q_s \\ q_c \end{Bmatrix}$$

equation (1) can be written as

$$\left([M_s \mid M_c]s^2 + [2\zeta M\Omega \mid 0]s + [M_s\Omega^2 \mid M_c\Omega^2] + \frac{1}{2}\rho V^2[\hat{Q}_s \mid \hat{Q}_c]\right)\begin{Bmatrix} q_s \\ q_c \end{Bmatrix} = -\frac{1}{2}\rho V\{\hat{Q}_g\}w_g \qquad (2)$$

where the subscript s denotes a structural quantity and the subscript c, a control quantity. An equation that relates control-surface motion to wing response (feedback control) can be expressed as

$$\{q_c\} = [T][\varphi]\{q_s\} \qquad (3)$$

where [T] is a transfer function matrix and $[\varphi]$ is the matrix of modal displacements at the sensor locations. Typically, [T] is expressed as a rational polynomial in s by letting

$$[T] = \frac{[T_N]}{Q(s)}$$

where Q (s) is a scalar polynomial representing the common denominator of all the elements of [T], and $[T_N]$ is a matrix of the resulting numerators. Equation (3) can then be expressed as

$$\{q_c\} = \frac{[T_N][\varphi]}{Q(s)}\{q_s\} \qquad (4)$$

Typically, the elements of the aerodynamic matrices $\hat{Q}_s, \hat{Q}_c, \hat{Q}_g$ are available as tabular functions of reduced frequency k, whereas the control law is expressed in terms of a rational polynomial in the Laplace variable s. To combine unsteady aerodynamic forces with structures and controls the concept of analytic continuation for the unsteady aerodynamics was developed[5,6]. Using this method the variation of the aerodynamic matrices with s can be approximated by the representation

$$[\hat{Q}] = [A_0] + [A_1]\left(\frac{b}{V}\right)s + [A_2]\left(\frac{b}{V}\right)^2 s^2 + \sum_{i=3}^{n_l} \frac{[A_i]s}{\left(s + \frac{V}{b}\beta_{i-2}\right)} \qquad (5)$$

where $[\hat{Q}]$ is $\hat{Q}_s, \hat{Q}_c, \hat{Q}_g$, n_l is the number of aerodynamic lag terms β, and all of the matrix coefficients and β values are real. Substitution of equations (4) and (5) into equation (2) and multiplication by Q (s) yields a matrix polynomial expression in s of the form

$$\left([F_0] + [F_1]s + [F_2]s^2 + \ldots + [F_m]s^m\right)\{q_s\} = \left(\{G_0\} + \{G_1\}s + \ldots + \{G_m\}s^m\right)w_g \qquad (6)$$

where the matrix coefficients $[F_i]$ and $\{G_i\}$ are functions of Mach number, velocity, and dynamic pressure. To conduct a stability analysis only the homogeneous part of equation (6) is solved; that is

$$\left([F_0] + [F_1]s + [F_2]s^2 + \ldots + [F_m]s^m\right)\{q_s\} = 0 \qquad (7)$$

Equation (7) can be reduced to a set of first-order equations of the form

$$s\{x\} = [A]\{x\} \qquad (8)$$

where the eigenvalues of [A] in equation (8) are the roots of equation (7). In order to determine the stability characteristics of the controlled aircraft, a root loci can be constructed at a given Mach number that corresponds to the variation in the eigenvalues of the system described by equation (8) as a function of dynamic pressure.

The modal response of the system per unit of gust velocity can be determined as a function of frequency by solving equation (6) at discrete values of ω, for $s = i\omega$; that is

$$\frac{\{q_s(s)\}}{w_g} = \left([F_0] + [F_1]s + [F_2]s^2 + \ldots + [F_m]s^m\right)^{-1} X\left(\{G_0\} + \{G_1\}s + \ldots + \{G_m\}s^m\right) \qquad (9)$$

Using equation (4), the control-surface response can then be evaluated by

$$\frac{\{q_c(i\omega)\}}{w_g} = \frac{[T_N][\varphi]}{Q(i\omega)}\frac{\{q_s(i\omega)\}}{w_g} \qquad (10)$$

This form of the equations of motion can be used to evaluate frequency and power-spectral-density responses.

ISAC - Interaction of Structures, Aerodynamics, and Controls

The capability detailed above has been incorporated in a computer program identified by the acronym ISAC. Much of the analysis performed on active control systems at NASA Langley is done using ISAC. The system, as detailed in figure 2, is an assembly of several programs tied together through a common data complex.

Modal characteristics of flexible aircraft are determined outside of ISAC by a suitable structural vibration analysis program. Modal deflections and slopes are then interpolated within ISAC to points required by the unsteady aerodynamics code or to sensor locations. The Doublet Lattice aerodynamics code is built into the program, however, unsteady aerodynamic forces may be input into the program from a separate source.

The equations of motion are represented in either the frequency domain or in the state-space formulation. Sensor, actuator, and controller dynamics can be characterized either in terms of transfer matrices or corresponding state-space representation. The basic types of dynamic response performed within ISAC include stability, deterministic responses such as frequency responses and time histories, and stochastic responses such as rms values of controlled response due to a unit rms gust velocity or control surface deflection. PSD plots of the frequency response output may also be determined. Typical

example output is presented in figure 3.

Unsteady Aerodynamic Force Approximations

The motivation for expressing the aerodynamic forces as a function of s, as given by equation (5), is to enable the equations of motion to be transformed into a set of linear time invariant state space equations of the form $\dot{x} = Ax + Bu$. When the approximation given by equation (5) is used, the resulting state space equations include augmented states which correspond to the aerodynamic lag terms $\left(s + \frac{V}{b}\beta_{i-2}\right)$. The number of augmented states is a function of the number of denominator roots in the approximation. For example, the least-squares approximation given in equation (5) results in a number of aerodynamic states which is the product of the number of lag terms and the number of modes. This approximation can yield large systems of equations to be solved.

The ISAC computer program has implemented three methods for performing aerodynamic approximations[7]. These are the least-squares method[5,6] and the modified matrix-Pade' method[8], which are of the form of equation (5), and the minimum-state method[9]. Each of these methods results in a progressively lower number of aerodynamic states in the equations of motion but with a greater computational cost to determine the approximation. Reducing the number of differential equations when approximating the unsteady aerodynamics significantly reduces the computer time and cost to perform aeroservoelastic analysis, in particular real-time simulation studies, as well as allowing larger problems to be analyzed. Figure 4 compares the three methods in terms of the total approximation error versus the number of aerodynamic state equations.

Unsteady Aerodynamic Correction Factor Methods

Correction factor methods[10] are being developed which use steady experimental or analytical pressure or force data to correct steady and unsteady aerodynamic calculations. The motivation for this work is to improve the accuracy of routine analytical calculations using high quality aerodynamic data. Correction factors are multipliers which are applied to aerodynamic downwashes or pressures in aerodynamic calculations to improve their applicability. This methodology is currently being used to improve the accuracy of the Doublet Lattice Method (DLM) unsteady aerodynamic code used in the ISAC program.

Three different approaches to calculate the correction factors are being developed and implemented. The first approach is to require a match between analytical and experimental surface pressure distributions, the second approach requires airfoil section characteristics to be matched and the third matches total aircraft force, derivative, or integrated pressure data. The first and second approaches require interpolation of the known aerodynamic data to essential analysis points. For the first approach the correction factors are calculated as the ratio of experimental to analytical pressure coefficients at discrete points on the wing. The second approach is similar but the correction factors are ratios of section properties, such as C_{l_α}, C_{m_α}, etc. Optionally, optimization techniques can be used to determine correction factors which minimize section property errors and/or minimize the change in the analytical pressure distribution. The third approach also uses optimization techniques to determine correction factors so that total aircraft analytical forces, moments, or control derivatives more nearly match known data.

The pressure distribution matching approach has been implemented and applied to a rectangular supercritical wing that was tested previously in the Langley Transonic Dynamics Tunnel[11]. Unsteady aerodynamic pressures were calculated using the Doublet Lattice Method to determine oscillatory aerodynamics at reduced frequencies corresponding to those where wind tunnel data was taken. Figure 5 shows a comparison of unsteady experimental pressure data and uncorrected and corrected analytical data for two reduced frequencies at Mach 0.4. Both downwash and pressure correction factors resulted in improved prediction of the pressure magnitudes on the leading edge of the airfoil, with mixed results farther aft where the magnitudes are much smaller. The effect of downwash correction factors on phase is generally beneficial, with poorer results in the same regions as for the pressure magnitudes.

Synthesis

In addition to analysis, the development of control law design methodology has been an integral part of the NASA Langley research program. The control law design process is presented in figure 6. Several approaches to the control law synthesis block are available at NASA Langley, ranging from the application of "classical" control theory to the use of "optimal" methods. Classical techniques are based on root locus and Bode' type analyses and have been applied primarily to single-input, single-output systems. Optimal methods provide an excellent basis for the systematic approach to the control law synthesis problem and are extremely attractive for the multiple-input, multiple-output problems. Therefore, considerable attention has being given to design methods that employ this approach.

The Linear-Quadratic-Gaussian (LQG) Method has become a widely accepted means of synthesizing optimal controllers. The theory is based on the design of a controller which minimizes a performance function. Since the performance function can be defined in terms of such quantities as control deflection, bending moment, accelerations, etc., the method can be adapted quite easily to numerous control tasks such as maneuver-load control, flutter suppression, and gust-load alleviation.

To find the optimal full-state feedback control law, the quadratic cost function

$$J = E\ [y^T Q y + u^T R u] \qquad (11)$$

is minimized where y is the output vector, u is the input vector, Q and R are weighting matrices, and E is the expected value operator. This leads to a control law of the form

$$u = -K x \qquad (12)$$

where K is the full-state feedback gain matrix and x is the vector of state variable estimates. Since the direct measurement of all state variables is not feasible, a Kalman Filter estimator must be designed and used to estimate the state variables from available measurements. The Kalman Filter along with the full-state feedback gain matrix constitute the optimal controller.

A shortcoming of optimal LQG methods, in particular for high-order systems which are characteristic of flexible airplanes, is the requirement that the controller be of the same order as the system being modeled. Not only is this unnecessarily complex, but the full-order controller is often very sensitive to small changes in system parameters. The standard method to reduce the order of the LQG controller is to construct lower-order controllers through truncation or residualization of the Kalman Filter. Several researchers[12,13,14] have shown that a reduced-order controller that approximates the full-order controller can be

found with little degradation in performance.

NASA Langley research in the area of optimal methods has included (1) the direct design of low-order optimal control laws using nonlinear programming techniques to search for values of the controller which minimize the performance, (2) the application of the method of Doyle and Stein[15] to improve stability margins during estimator design for aeroservoelastic problems, and (3) the use of nonlinear programming techniques to impose inequality constraints such as rate limits, loads, etc., on the optimization process resulting in constrained optimal-control laws. An example of how a modified LQG method is applied to the design of a flutter suppression system is presented in reference 14.

Digital Control Law Synthesis

Because of flexibility and cost effectiveness the implementation of active control laws on digital microprocessors is becoming more common. If the sample rate of such sampled-data systems is sufficiently high, the synthesis procedures described earlier can be accomplished using analog methods and then discretized for digital implementation. However, the direct synthesis and simulation of digital control laws, which includes the effect of sampling rate, computational delay, anti-aliasing filters, etc., will reduce problems associated with the digital implementation of analog designs.

Reference 16 presents a direct digital control law synthesis procedure using constrained optimization. The objective is to develop methodology for the direct synthesis of digital active control laws for aeroservoelastic systems, which meet multiple design requirements while maintaining reasonable stability margins. In the reference, the system is mathematically modeled by a set of discrete state-space equations at a specified sampling rate. An LQG-type cost function consisting of the weighted sum of steady state responses is minimized by updating free parameters of the digital control law while satisfying a set of constraints on the design loads and responses. The general expressions for the gradient of the cost function and the constraints are derived analytically. The designer can choose the structure of the initial control law and design variables, hence, existing control laws as well as full- or reduced-order LQG control laws can be modified to meet specific design objectives.

The methodology presented in reference 16 was used to synthesize second-order digital control laws for gust-load alleviation of a drone aircraft modeled by a 32nd order sampled data system (see figure 7). The objective was to design a low order, digital, gust-load alleviation (GLA) control law that would reduce by one half the open loop RMS values of wing-root bending moment and shear due to a Von Karman gust spectrum, without increasing the RMS outboard bending moment and torsion. The outboard ailerons and the elevator were used for control inputs. Accelerometers located near the ailerons and near the fuselage center of gravity were used as measurement outputs. The equations of motion were expressed as a 32nd order state-space model which included rigid-body plunge rate, pitch and pitch rate, three flexible wing modes, ten unsteady aerodynamic lag states, a first-order elevator actuator dynamics term with a 100 Hz double-pole filter, an eighth-order aileron actuator dynamics term, and a second-order Dryden gust spectrum.

Five control laws were synthesized. First, an LQG optimal control law was synthesized in analog form assuming all the states could be measured directly. The corresponding RMS values are given in table 1. Since all the states were not available for feedback, a 32nd order Kalman state estimator was also designed. The closed-loop responses for the control law with Kalman Filter are higher, as given in table 1, but they satisfy the design requirements. The 32nd order Kalman Filter control law was then truncated to second order by retaining only the key states corresponding to pitch angle and pitch rate. This second-order control law was discretized using Z-transform methods with a zeroth-order hold, at 100 samples per second. The RMS response values of the resulting digital control law, referred to as control law I, are presented in the table. Although the root bending moment and torsion were reduced by nearly 40 percent, the outboard bending moment increased substantially. Three of the four design objectives were not met. With control law I as a starting point, an unconstrained optimization was performed using the same LQG cost function as in the full-state continuous case. The optimized control law, referred to as control law II, met all design requirements except a very slight increase in outboard bending moment. This was accomplished by a greater sharing of control law activity between the elevator and the aileron. To prevent the slight increase in the outboard bending moment, a constrained optimization procedure was attempted next using control law II as a starting point. The RMS outboard bending moment was treated as a constraint (fixed at 96 percent of open loop) instead of being weighted in the cost function. The results for the optimized control law, designated control law III, are presented in the table. All design objectives were met.

Integrated Design

Although more and more active control concepts are being introduced into flight systems the greatest potential benefits will accrue only when they are considered as part of an integrated design process which includes aerodynamics, controls, structures, and propulsion in the preliminary design phase as shown in figure 8.

The state of the art in aeroservoelastic analysis is now at the point where it is possible to accurately predict aeroservoelastic interactions. The next logical step is to develop design methodologies which use aeroservoelastic interactions to improve aircraft performance. NASA Langley research is aimed at developing this integrated methodology. An integrated design methodology which considers only structures and controls is now being investigated based on the hierarchal multilevel problem decomposition and optimization techniques[17]. This approach breaks the integrated-design problem into a hierarchal structure that allows for a natural ordering of design objectives into system-level objectives and subordinate subsystem objectives. This ordering provides a framework within the design methodology to tradeoff subsystem performance (e.g. structural weight versus control surface deflections) for improved system performance. A rational means for making subsystem performance tradeoffs is provided through the use of optimization techniques and sensitivity of optimum solution concepts to obtain the sensitivity of the optimal subsystem designs to fixed parameters. The subsystem design sensitivity information is used at the system-design level to select the fixed parameters so as to influence the subsystem designs in such a way that overall system performance is improved.

The approach described above is illustrated in figure 9. Control law and structure designs occur simultaneously and in parallel with the recognition that the two disciplines interact in the actual aircraft. These designs proceed on the basis of the individual discipline design objectives and variables. The sensitivity of the optimum control design to the structural element sizes, and the sensitivity of the optimum structural design to the control law gains are then computed and passed on to the system level. This sensitivity information is used as gradient information at the higher level to determine the most effective tradeoffs to achieve the desired system performance.

The concept of the sensitivity of an optimum solution to problem parameters which were held fixed during an optimization process is illustrated in figure 10. Consider an optimization problem where an objective function J(u,p) is to

be minimized by choice of a design variable u, with some design parameter p held constant at some nominal value p_0. For a different nominal value (p_1) the optimum value will be different. The sensitivity of the optimum solution with respect to the design parameter p is then the change of the optimum value of the objective function and the change of the design variable at the optimum due to changes in the parameter. Analytical expressions for the sensitivity of the optimal solution to the parameter p can be derived from the necessary conditions of optimality for the problem.

The analytical sensitivity of the optimized structural-design solution has been developed and reported elsewhere by other researchers in the field. The sensitivity of the optimal LQG control laws to LQG problem-formulation parameters and structural-design parameters (for structural systems) are calculated using analytical sensitivity equations without multiple perturbed LQG solutions and finite differencing. The use of analytical sensitivity expressions results in a significant decrease in the computation burden required for the integrated structure/control law design method outlined above and yields accurate sensitivity information. Sensitivity of the LQG solution to structural parameters permits tailoring the structural design to improve the control subsystem (and also overall system) performance.

Numerical results have been calculated for an example problem as shown in figure 11. This application involves the design of an optimal LQG control law and the prediction of changes in the optimally-controlled response of the vehicle due to changes in the first wing-bending natural frequency. Changes in the mean-square wing-tip acceleration and the mean-square aileron-deflection rate due to changes in wing first bending frequency for a random gust environment are shown in the figure. The lines show the predicted change in performance if a new optimal control law was implemented for changes in the frequency parameter. The symbols show the actual change in performance when the parameter was varied and the resulting new optimal control law was computed and implemented. For a ± 10% variation in the wing first bending frequency the sensitivity predictions were reasonably accurate. For larger variations the predictions were not as accurate, but the trends were correct.

Continued development of the integrated structure/control law design methodology will proceed along two lines: a) derivation of analytical sensitivity expressions for reduced-order, constrained optimal control law problems reflecting a more realistic control law design methodology and b) exercising the complete design methodology with structural optimization and the LQG control law problem formulation.

Wind-Tunnel Studies

Aeroelastic models are used to obtain experimental results at conditions where analytical results are known to be inaccurate or totally unavailable or where flight testing would be extremely hazardous. Model results can be obtained in a more timely manner than flight results, are more cost effective, and are more amenable to extensive parametric studies. In many cases model tests are the most timely and economical means for establishing proof of concept and for generating experimental data for comparison with analysis. As a result, wind-tunnel testing of aeroelastic models has been a cornerstone of the NASA Langley aeroservoelasticity research program. It is worth noting that the first successful demonstration of flutter suppression in the United States was accomplished in the Langley Research Center Transonic Dynamics Tunnel using a simplified model of a supersonic transport wing[18]. A major contribution from these tests was the successful design and fabrication of miniature hydraulic actuators, similar to that shown in figure 12, that paved the way for future wind-tunnel studies using active controls.

The initial objectives of the early wind-tunnel studies were to demonstrate the feasibility of active control concepts and to assess their effectiveness. Later studies began to deal with "engineering" aspects such as the effect of failed actuators and the effect of switching from analog to digital computers. A series of pioneering wind-tunnel studies, as shown in figure 13, did much to advance active controls technology by demonstrating the ability not only to control aeroelastic response but to also predict system performance. Some of the more recent wind-tunnel studies are described below.

Adaptive Flutter Suppression

Modern fighter aircraft carry a large variety of external wing-mounted stores. In some instances it is necessary to placard (restrict) the operational envelope of the aircraft because of store flutter. One approach to avoiding this restriction is to use an active control system to suppress the flutter. Adaptive control systems are particularly attractive for this application because no knowledge of the store configuration being flown is required. Adaptive control systems continually monitor the state of the system by measuring system responses due to control inputs and continually update control laws based on these measurements.

A 1/4-scale, cable-mounted, full-span F-16 aeroelastic model equipped with an Adaptive Flutter Suppression System (AFSS) was tested in the Transonic Dynamics Tunnel in a joint USAF/General Dynamics/NASA test. A photograph of the model mounted in the wind tunnel is shown in figure 14. The AFSS was implemented on a digital computer that was located in the tunnel control room. Accelerometers were used to measure the wing motion, and the flaperon control surfaces were used to suppress the flutter.

An overview of the operation of the controller is presented in figure 15. The flutter model is represented by the block labeled "Plant." Computer-generated random excitation signals, u, were sent to the flaperons to provide a continuous low-amplitude random-excitation to the plant. The output response from three accelerometer pairs located on the left and right wing is sampled at a rate of 100 samples/second. The block labeled "Identified Plant" uses the sampled input, u, and output, y, to identify a state-space representation of the wind-tunnel model. The state-space model matrices are supplied to a linear quadratic control algorithm which develops a control law to suppress flutter of the identified plant. The control law is then transferred to the AFSS controller which generates the feedback signal. The feedback signal is the product of the control law and the current state vector. When the control law is sent to the the controller, the identification and control calculations are repeated. The identified plant, JK matrix, and the control law were updated at a rate of approximately one/second. The state vector and feedback signal are updated at a rate of 100 times/second.

Flutter data, AFSS off and AFSS on, were obtained for three critical-store configurations. Basic systems-on testing began below the flutter boundary and proceeded above the system-off flutter boundary. The adaptive control law updated up to 2500 times during a test pass without failing to suppress flutter. For two store configurations (one with mild flutter onset, the other with moderate flutter onset) a 30-percent increase in flutter speed was demonstrated; for the third configuration (violent flutter onset) an 18.5-percent increase in flutter speed was obtained. The results for the three store configurations are given in figure 16. In addition to the basic testing, the system was evaluated using actual store drops where wing-tip missiles were ejected during testing to cause the model to change rapidly from a stable, flutter-free configuration to an unstable, flutter configuration. The AFSS quickly recognized that the dynamics of the model had changed and updated the control law to suppress the flutter.

Active Flexible Wing

In support of integrated aeroservoelastic design, Rockwell International Corporation has developed a concept referred to as the Active Flexible Wing (AFW). This concept uses wing flexibility and multiple control surfaces to vary the wing shape resulting in improved performance and reduced structural weight.

AFW Model

Under a joint Rockwell/Air Force/NASA program, Rockwell designed and built an aeroelastic model to be tested in the Langley Transonic Dynamics Tunnel (TDT). A photograph of the model in the TDT is shown in figure 17. The model has a span of about 9 feet and is mounted on a sting such that it is free to roll. The model consists of a rigid fuselage and flexible wings and has no horizontal tails. Some aeroelastic tailoring was employed to provide desired amounts of bending and twist as a function of aerodynamic load. The model has two leading-edge and two trailing-edge control surfaces on each wing panel, with each driven by miniature electrohydraulic actuators. The model was instrumented with a force balance, accelerometers, strain gauges, rotary displacement sensors, roll potentiometer, and a roll rate gyro. Figure 18 illustrates the location of the control surfaces and pertinent instrumentation.

AFW Control Law Design

NASA designed Active Roll Control (ARC) laws for two test conditions (M = .90, dynamic pressure = 150 psf; M = .90, dynamic pressure = 250 psf)[19]. The aeroelastic plant was represented by the rigid-body roll mode plus the first 10 antisymmetric flexible modes (see table 2). The actuators were represented by third-order transfer functions. Even though the control laws were implemented on a digital controller, the sampling rate was significantly high (200 samples/second) as compared to the key flexible modes so that the controller was assumed to be analog and the control laws were designed using classical analog methods.

A block diagram of the ARC system is shown in figure 19. At a dynamic pressure of 250 psf the trailing-edge inboard and the leading-edge outboard control surface were used. The design objectives of the ARC were to achieve a 90-percent roll angle in less than 0.40 second with a minimum of +6 db gain margin, ±40° phase margin. The feedback gains K_1 and K_2, the feedforward gains K_{c1} and K_{c2}, and the second-order filter constants ζ_n, and ω_n were determined by trial and error such that the design objectives were met.

Control Law Parameterization

The nominal ARC system has identical gains in each feedback loop ($K_1 = K_2 = .2$) and different but identical gains in each feedforward loop ($K_{c,1} = K_{c,2} = 1$). It was recognized that there are an infinite number of feedback gains and feedforward gains which result in the same closed-loop stability and performance but with different commanded control surface displacements. As a consequence, one pair of control surface deflections could be traded off against another pair with no change in performance or stability. This ability is especially beneficial when designing multiple active control functions that are to be used simultaneously.

By ignoring the stick-shaping filter, the anti-aliasing filter, and the second-order filter in figure 19, and using only the roll degree of freedom the following closed-loop transfer function can be obtained

$$\frac{p(s)}{p_c(s)} = \frac{K_{c_1}\hat{L}_{\delta_1} + K_{c_2}\hat{L}_{\delta_2}}{s + \hat{L}_p + K_1\hat{L}_{\delta_1} + K_2\hat{L}_{\delta_2}} \tag{13}$$

where p(s) is the roll-rate, $p_c(s)$ is the roll-rate command, $\hat{L}_p$ is the roll damping defined by $-\frac{L_p}{I_{xx}}$, and $\hat{L}_{\delta_i}$ is the dimensional roll effectiveness for the ith control pair and is defined by $\frac{L_{\delta_i}}{I_{xx}}$

Closed-loop stability remains constant if, for the denominator of (13),

$$\hat{L}_p + K_1\hat{L}_{\delta_1} + K_2\hat{L}_{\delta_2} = s' \tag{14}$$

(where s' is a constant). By inspection, the following linear equation may be written for K_2 as a function of K_1

$$K_2 = \frac{s' - \hat{L}_p}{\hat{L}_{\delta_2}} - \frac{\hat{L}_{\delta_1}}{\hat{L}_{\delta_2}} K_1 \tag{15}$$

All combinations of K_1 and K_2 which satisfy this equation result in a closed-loop system whose eigenvalue is located at s = - s'. Equation (15) can be parameterized by the term κ, where

$$K_1 = \frac{s' - \hat{L}_p}{\hat{L}_{\delta_1}}\,\kappa \tag{16}$$

$$K_2 = \frac{s' - \hat{L}_p}{\hat{L}_{\delta_2}}(1.0 - \kappa) \tag{17}$$

and κ varies between 0 and 1.0 κ = 0.76 corresponds to equal values of feedback gain.

In a similar manner the roll performance can be parameterized by arbitrarily setting the value of the numerator of equation (13) to the value which results when $K_{c_1} = K_{c_2} = K'_c$. Therefore,

$$K_{c_1}\hat{L}_{\delta_1} + K_{c_2}\hat{L}_{\delta_2} = K'_c\left(\hat{L}_{\delta_1} + \hat{L}_{\delta_2}\right) \tag{18}$$

and

$$K_{c_2} = \frac{K'_c}{L_{\delta_2}}\left(\hat{L}_{\delta_1} + \hat{L}_{\delta_2}\right) - K_{c_1}\frac{\hat{L}_{\delta_1}}{\hat{L}_{\delta_2}} \tag{19}$$

Picking a single parameter κ_c as before

$$K_{c_1} = \frac{K'_c \left(\hat{L}_{\delta_1} + \hat{L}_{\delta_2} \right)}{\hat{L}_{\delta_1}} \kappa_c \qquad (20)$$

and

$$K_{c_2} = \frac{K'_c \left(\hat{L}_{\delta_1} + \hat{L}_{\delta_2} \right)}{\hat{L}_{\delta_2}} (1.0 - \kappa_c) \qquad (21)$$

$\kappa_c = 0.76$ yields equal values of gain in the forward path.

Figure 20 presents analytical time histories of δ_2 (LEO) deflecting in response to a 0.30-second roll-rate command for three values of feedforward gain κ ($\kappa_c = 0.76$). These results are for s' = 26.0, and time to roll 90 degrees relaxed to 1.5 seconds to stay within the linear range of the control surfaces. The maximum values of δ_2 are indicated by the open symbols.

Figure 21 presents time histories of δ_2 (LEO) deflecting in response to a 0.30-second roll-rate command for three values of feedback gain κ_c ($\kappa = 0.76$). The maximum values of δ_2 are indicated by the closed symbols. It can be seen that the character and magnitude of the deflection time histories change significantly with κ and κ_c while holding stability and performance constant.

Wind-Tunnel Results

To validate the analysis predicted by control law parameterization, time responses were obtained for several values of κ and κ_c. Figure 22 contains a comparison of maximum values of δ_1 (TEI) and δ_2 (LEO) as a function of κ and κ_c at a Mach number of 0.90 and a dynamic pressure of 250 psf. The solid and dashed lines correspond to analytical predictions of δ_{1max} and δ_{2max}, respectively. It can be seen that the behavior is well predicted by analysis.

Concluding Remarks

The achievements that have been made in the control of aeroelastic response are impressive, but so are the outstanding needs. More than ever the role that aeroservoelasticity plays in the design of aerospace vehicles is becoming important to the success of innovative configurations required to eke out the greatest possible performance for an increasingly varied spectrum of missions. Almost from the inception of powered flight, the aeroelastic characteristics of a design have been considered on the negative side of the ledger. A revolution is beginning to occur in the perception of aeroelasticity - from that of a problem child to be dealt with to that of a "knight in shining armor" capable of wresting increased performance from configurations undreamed of a few years ago. This is made possible by the recognition of the need for a close working alliance between aeroelasticity, structures, and stability and control specialists very early in the design process. With this approach we see desired flexibilities being designed into new configurations and naturally unstable designs being accepted on the premise that "active controls" will make things right.

Acknowledgment

The authors wish to acknowledge the work of the members of the Aeroservoelasticity Branch at NASA Langley Research Center whose research is being overviewed in this paper. Contributions are included from Mr. B. Perry III, Ms. S. Tiffany, Mr. M. Gilbert, and Ms. C. Wieseman. In addition, the authors wish to acknowledge the work of Dr. V. Mukhopdhyay of the Aerospace Technologies Division of PRC, Hampton, Virginia, for his contributions.

References

1. Zbrozek, J.; Smith, K. W.; and White, D.: Preliminary Report on a Gust Alleviator Investigation on a Lancaster Aircraft. ARC R and M No. 2972, August 1953.

2. Hunter, Paul A.; Kraft, Christopher C.; and Alford, William L.: A Flight Investigation of an Automatic Gust-Alleviation System in a Transport Airplane. NASA TN D-532, January 1961.

3. Bisplinghoff, R. L.; Ashley, H.; and Halfman, R. L.: Aeroelasticity. Addison-Wesley, Cambridge, 1955.

4. Johannes, R. P.; Burris, P. M.; and Dempster, J. B.: Flight Testing Structural Performance of the LAMS Flight Control System. AIAA Paper No. 68-1067, 1968.

5. Roger, Kenneth L.: Airplane Math Modeling Methods for Active Control Design. Structural Aspects of Active Controls, AGARD-CP-228, August 1977.

6. Abel, I.: An Analytical Technique for Predicting the Characteristics of a Flexible Wing with an Active Flutter Suppression System and Comparison with Wind Tunnel Data. NASA TP-1367, February 1979.

7. Tiffany, S. H.; and Adams, W. M., Jr.: Nonlinear Programming Extensions to Rational Function Approximations of Unsteady Aerodynamics. AIAA Paper No. 87-0854, April 1987.

8. Vepa, R.: Finite State Modeling of Aeroelastic Systems. NASA CR 2770, 1977.

9. Karpel, M.: Design for Active and Passive Flutter Suppression and Gust Alleviation. NASA CR 3482, November 1981.

10. Wieseman, C. D.: Methodology for Matching Experimental and Analytical Data. AIAA Paper No. 88-2392, April 1988.

11. Ricketts, R. H.; Watson, J. J.; Sandford, M. C.; and Seidel, D. A.: Subsonic and Transonic Unsteady- and Steady-Pressure Measurements on a Rectangular Supercritical Wing Oscillated in Pitch. NASA TM-85765, August 1984.

12. Gangsaas, D.; and Ly, U.: Application of a Modified Linear Quadratic Gaussian Design to Active Control of a Transport Airplane. AIAA Paper No. 79-1746, August 1979.

13. Mahesh, J. K.; Stone, C. R.; Garrard, W. L.; and Dunn, H. J.: Control Law Synthesis for Flutter Suppression Using Linear Quadratic-Gaussian Theory. Journal of Guidance and Control, July-August 1981.

14. Mukhopadhyay, V.; Newsom, J. R.; and Abel, I.: A Method for Obtaining Reduced-Order Control Laws for High-Order Systems Using Optimization Methods. NASA TP-1876, August 1981.

15. Doyle, J. C.; and Stein, G.: Robustness with Observers. IEEE Trans. Automated Control, Volume AC-24, August 1979.

16. Mukhopadhyay, V.: Digital Robust Active Control Law Synthesis for Large Order Systems Using Constrained Optimization. AIAA Paper No. 87-2588, August 1987.

17. Gilbert, M. G.: A Sensitivity Method for Integrated Structure/Active Control Law Design. NASA CP-2457, September 1986.

18. Sandford, M. C.; Abel, I.; and Gray, D.: Development and Demonstration of a Flutter Suppression System Using Active Control Laws. NASA TR R-450, December 1975.

19. Perry, B. P., III; Dunn, H. J.; and Sandford, M. C.: Control Law Parameterization for an Aeroelastic Wind-Tunnel Model Equipped with an Active Roll Control System and Comparison with Experiment. AIAA Paper No. 88-2211, April 1988.

Table 1.- Root mean square wing loads as percentages of open loop values and control surface activities as percentages of maximum allowed due to a unit RMS gust for Drone aircraft.

Design (order)	RMS loads on wing due to unit Dryden gust (% of open loop)				RMS control deflection and rate (% of maximum allowed)			
	Wing root		Wing outboard		Elevator		Aileron	
	BM	Shear	BM	Torsion	δ_1	$\dot{\delta}_1$	δ_2	$\dot{\delta}_2$
Open loop	100	100	100	100	0	0	0	0
Full state	26	25	23	17	49	6	35	32
Kalman fil.	49	49	81	57	20	3	13	9
Law-I (2)	63	60	140	63	13	1.5	51	10
Law-II (2)	43	43	101	66	25	1.7	25	1.3
Law-III(2)	45	45	92	62	33	3	5	1

Table 2.- Structural modes of AFW wind-tunnel model.

Mode	Description	Frequency, Hz
1	Sting 1st bending	7.18
2	Wing 1st bending	12.83
3	Fuselage yaw	16.60
4	Wing 2nd bending	34.17
5	Wing 1st torsion	35.05
6	Wing/fuselage	38.59
7	Wing 3rd bending	47.96
8	Wing bending/torsion	51.10
9	Wing 2nd torsion	53.03
10	Wing/fuselage	56.99

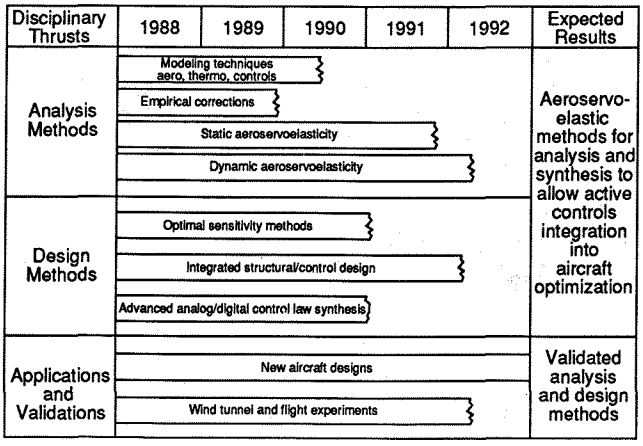

Figure 1.- Aeroservoelasticity five year plan.

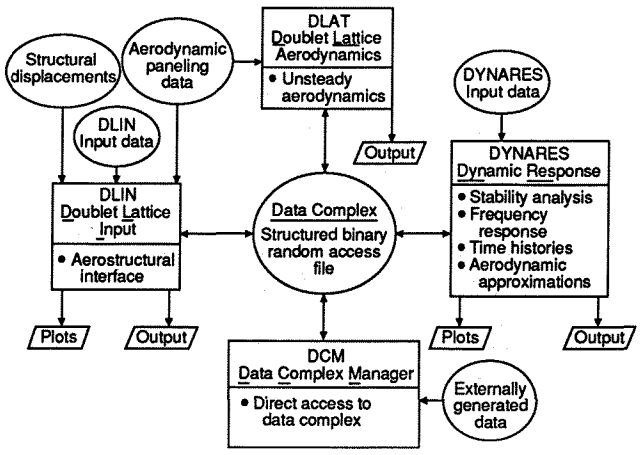

Figure 2.- Schematic of ISAC system.

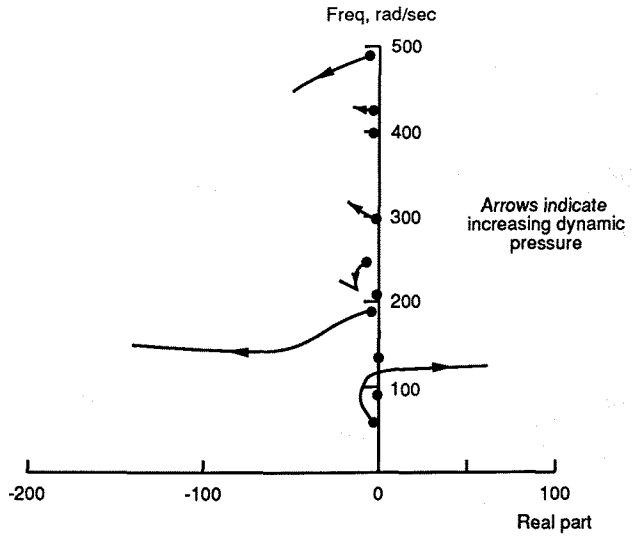

Fig. 3 (a) Dynamic Pressure Root Locus

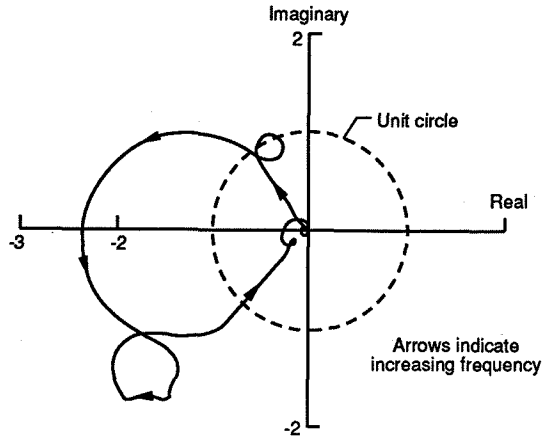

Fig. 3 (b) Nyquist Diagram

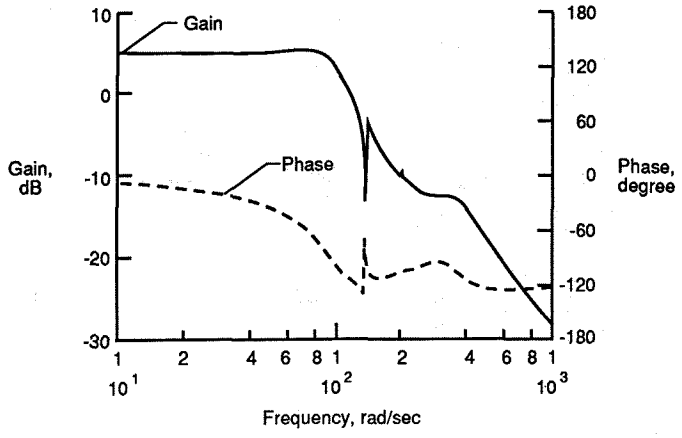

Fig. 3 (c) Bode' Plot

Figure 3.- Typical ISAC output.

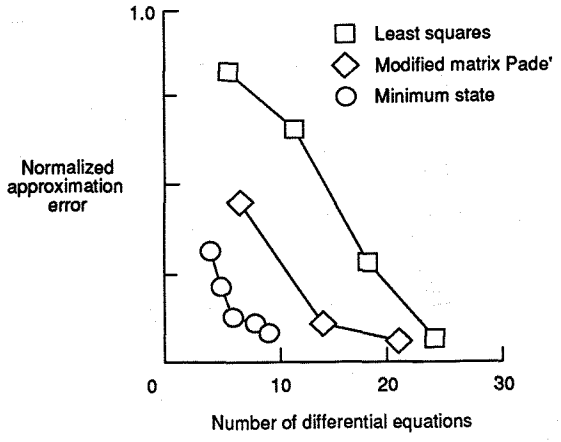

Figure 4.- Aerodynamic approximation error.

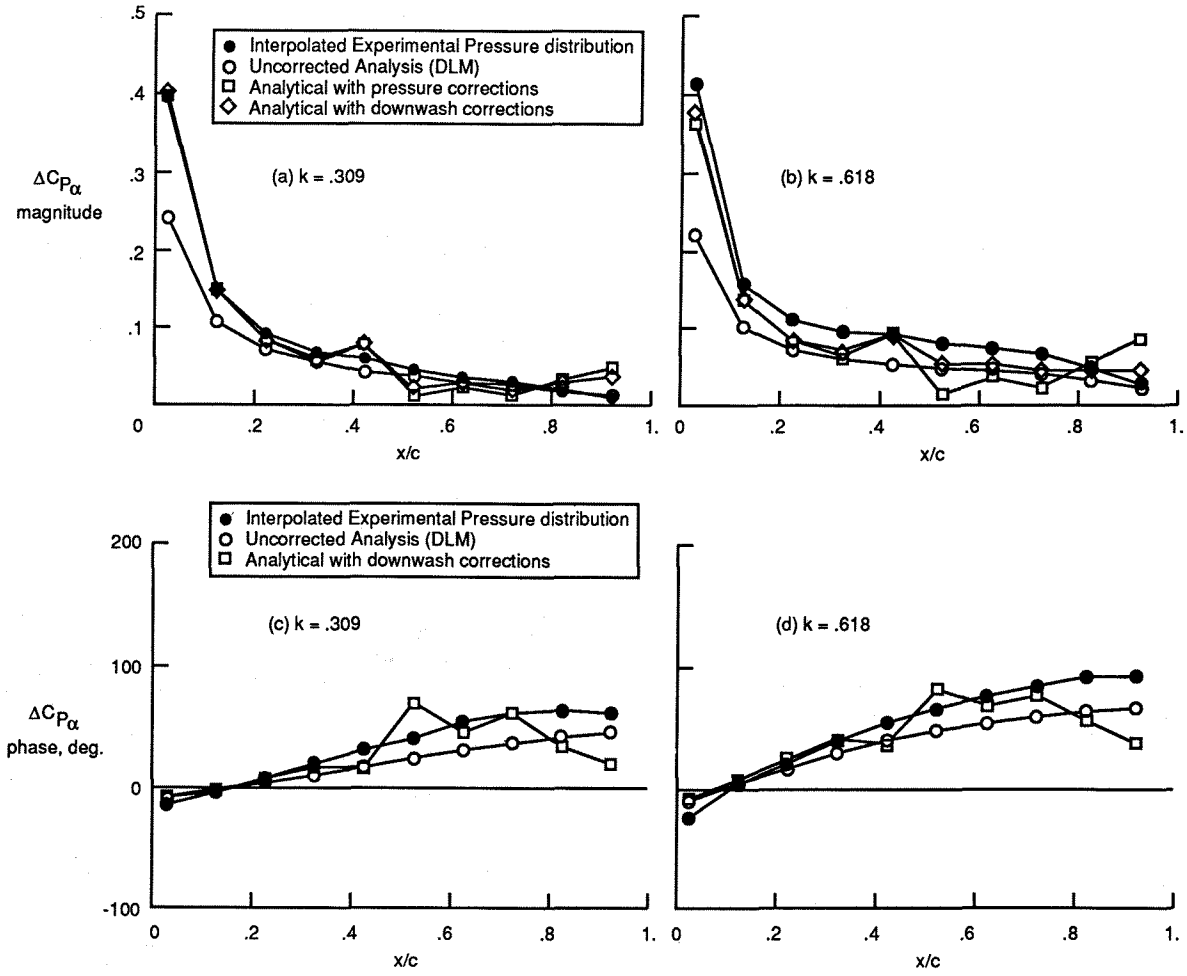

Figure 5. Comparison of corrected and uncorrected data at M=0.4.

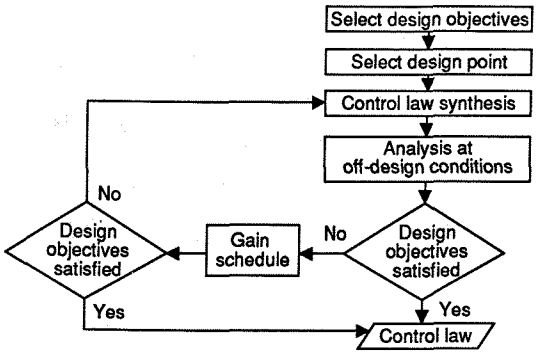

Figure 6.- Flow chart of control law design process.

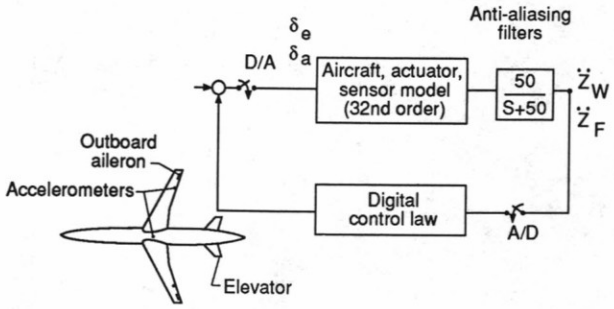

Figure 7.- Digital control law synthesis example problem.

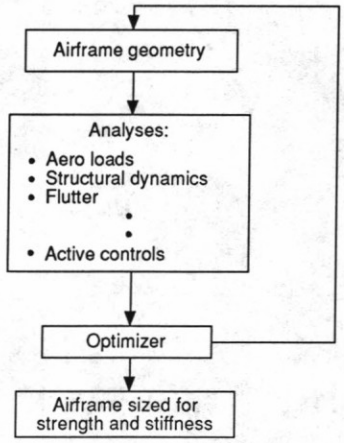

Figure 8.- Integrated design approach.

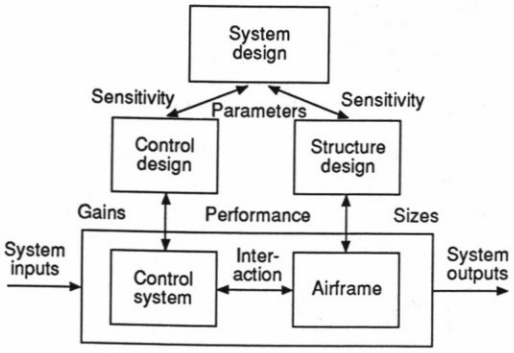

Figure 9.- Integrated structure/control design.

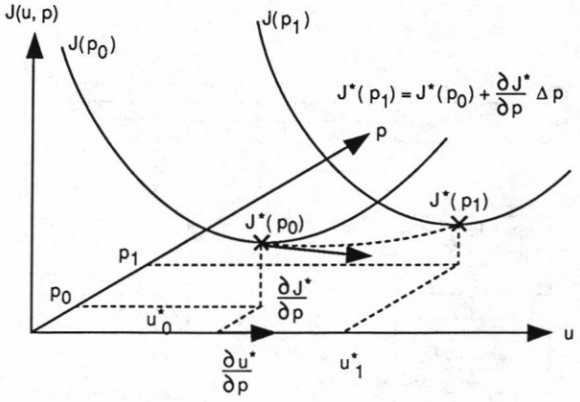

Figure 10.- Geometrical interpretation of optimum sensitivity.

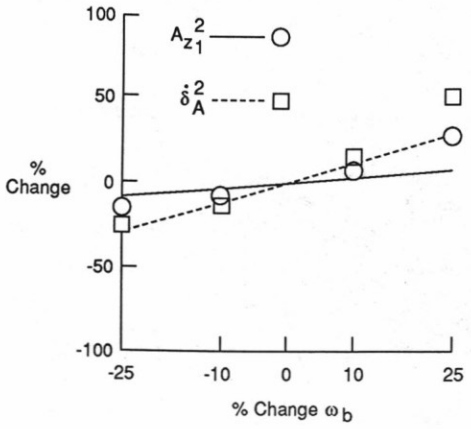

Figure 11.- Comparison of predicted and actual changes.

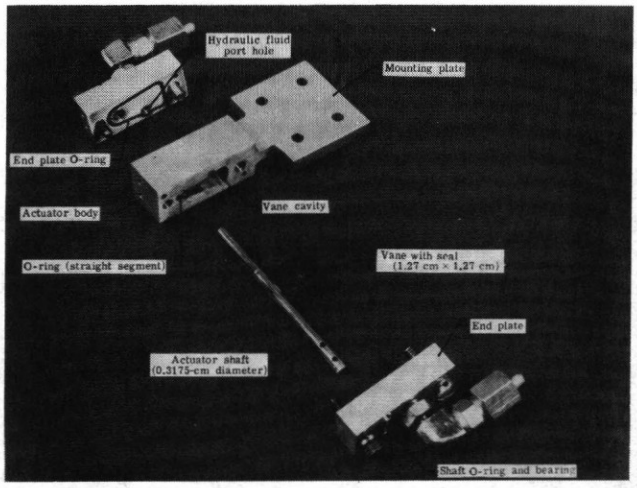

Figure 12.- Miniature hydraulic actuator components.

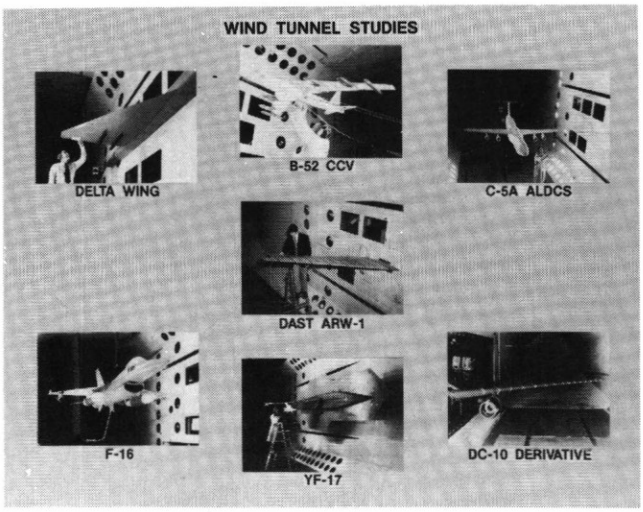

Figure 13.- Wind-tunnel studies.

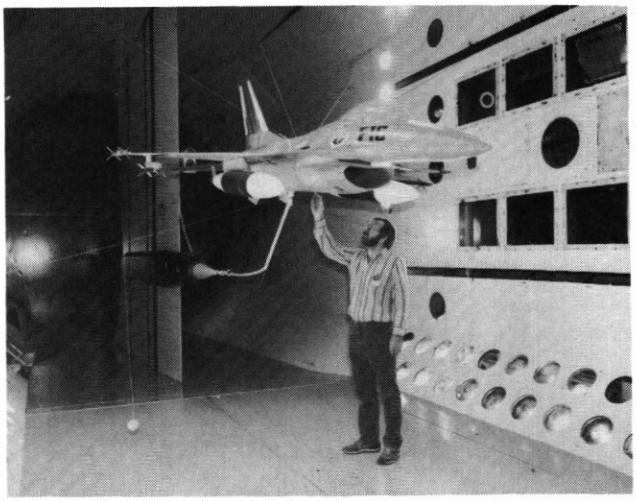

Figure 14.- F-16 adaptive flutter suppression model in Transonic Dynamics Tunnel.

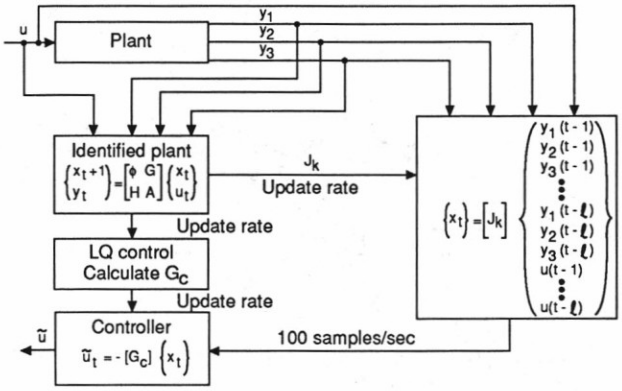

Figure 15.- Adaptive flutter suppression identifier and controller.

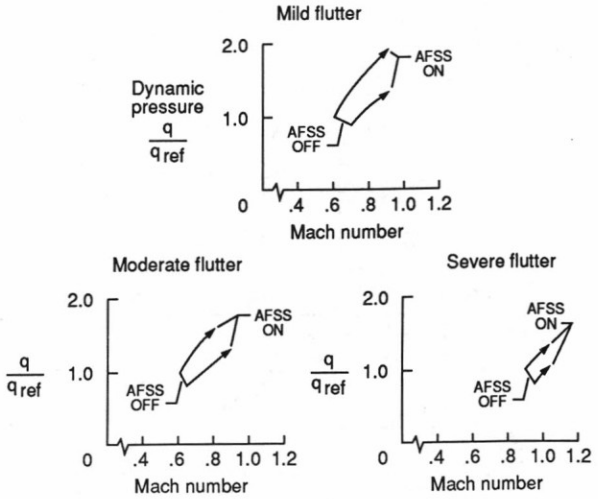

Figure 16.- Adaptive flutter suppression experimental results.

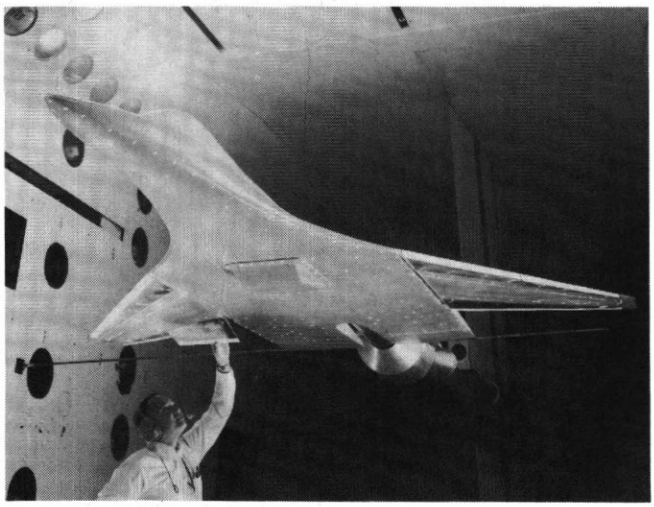

Figure 17.- AFW wind-tunnel model in Transonic Dynamics Tunnel.

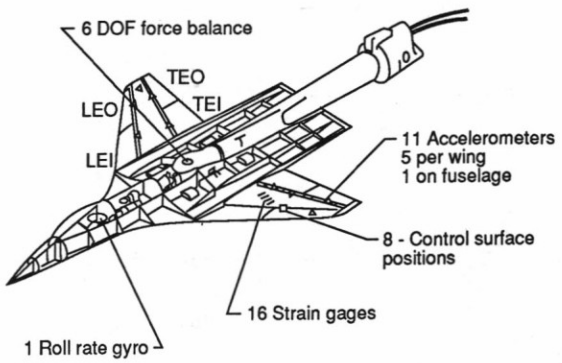

Figure 18.- Wind-tunnel model instrumentation.

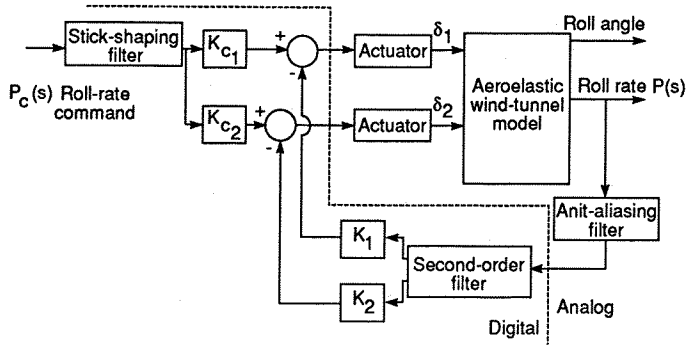

Figure 19.- Block diagram of active roll control system.

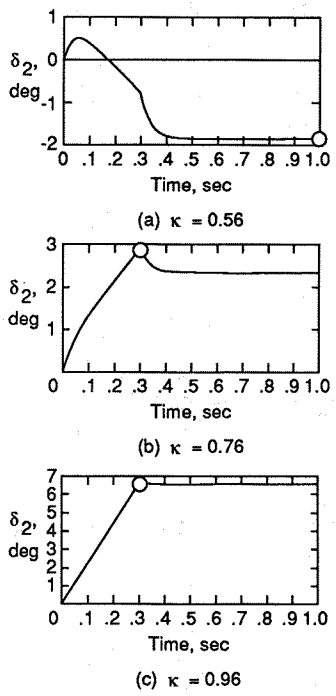

Figure 20.- Time histories of leading-edge outboard control surface deflections as a function of κ. κ_c=0.76.

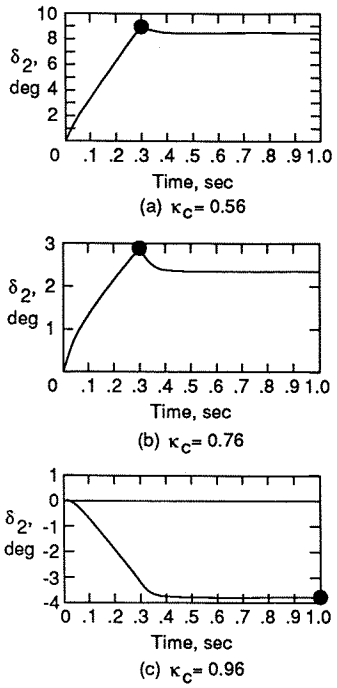

Figure 21.- Time histories of leading-edge outboard control surface deflections as a function of κ_c. κ=0.76.

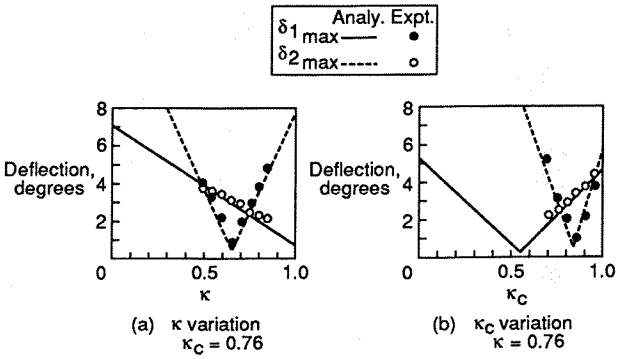

Figure 22.- Comparison of analytical and experimental parameterization results. Mach=0.9, dynamic pressure=250 psf.

Copyright © 1987 American Institute of Aeronautics and Astronautics, Inc. No copyright is asserted in the United States under Title 17, U.S. Code. The U.S. Government has a royalty-free license to exercise all rights under the copyright claimed herein for Governmental purposes. All other rights are reserved by the copyright owner.